Zhang *et al.*
EURASIP Journal on Advances in Signal Processing (2023) 2023:96
https://doi.org/10.1186/s13634-023-01058-3

EURASIP Journal on Advances in Signal Processing

RESEARCH Open Access

Modeling and analysis for group delay mismatch effect on wideband adaptive spatial interference cancellation

Yunshuo Zhang[1], Fangmin He[1*], Hongbo Liu[1], Yaxing Li[1], Zhong Yang[1], Ze Wang[1] and Jin Meng[1]

*Correspondence: hefangminemc@126.com

[1] National Key Laboratory of Electromagnetic Energy, Naval University of Engineering, Wuhan 430033, China

Abstract

The adaptive interference cancellation technique has been widely utilized in radar, GPS, data link, etc., systems to address challenges from external interference, such as co-site and hostile interference. Since the anti-jamming performance of the adaptive interference cancellation technique is sensitive to group delay mismatch between channels, the group delay mismatch becomes one of the main factors that limit the system's anti-jamming capability. However, the traditional adaptive interference cancellation system's mathematical model cannot quantitatively characterize the group delay mismatch effect on the wideband interference cancellation performance. In this paper, the mathematical model of the wideband adaptive spatial interference cancellation (ASIC) system is established, which considers the group delay mismatch, to quantitatively analyze the impact of group delay mismatch on the hostile interference cancellation. The mathematical model utilizes the weighted multi-tone signals to fit the wideband interference, and then, delay differences are attached to each tone signal to simulate the group delay mismatch. Then, the analytic expressions of weight and interference cancellation ratio are derived, which consider the interference bandwidth and group delay mismatch, to quantitatively analyze the group delay mismatch effect on the anti-jamming performance of the wideband ASIC system. Simulation results indicate that the theoretical analysis based on the mathematical model of wideband ASIC system are accurate, which can achieve the quantitative analysis of the group delay mismatch effect on the WIC performance.

Keywords: Group delay mismatch, Adaptive spatial interference cancellation, Wideband interference, Weight characteristics

1 Introduction

In space-limited platform and electronic warfare scenarios, the co-site interference and hostile interference submerge the desired signals of radar, GPS, data link, etc., systems over the entire bandwidth, which causes the interruption of the communication or target detection [1–5]. The co-site interference can be addressed by increasing the isolation between the transceiver antennas. However, the limited platform space restricts the isolation's optimization range [2]. Radar, GPS, data link, etc., systems also utilize spread

spectrum and frequency hopping techniques to resist hostile interference [6–9]. But the aforementioned passive anti-jamming methods are still challenging to counter the co-site interference with kilowatt (kW) power [10] and the hostile interference with megawatt (MW) power [11]. Therefore, active anti-jamming methods are required to address the challenges of external interference [12].

The adaptive interference cancellation technique is a typical active anti-jamming method, which is widely applied in various military platforms to improve the anti-jamming capability of systems [13]. The co-site interference can be suppressed by wired sampling from the interference source [14, 15] or utilize multi-sampling antennas to achieve the spatial selectivity of interference and desired signal and, thereafter, cancel the hostile interference [16–18]. However, the received interference is required to be filtered, amplified, and down-converted before anti-jamming processing [19, 20]. Since the anti-jamming performance of the adaptive interference cancellation technique is sensitive to group delay mismatch between channels, the group delay mismatch becomes one of the main factors that limit the system's anti-jamming capability [21]. Thus, when designing and implementing the adaptive interference cancellation system, it is necessary to quantitatively analyze the group delay mismatch effect on the wideband interference cancellation (WIC) performance and then constrain the group delay consistency between channels to meet the requirement of the anti-jamming capability improvement.

The definitions of group delay mismatch in the mathematical models of the adaptive interference cancellation systems are divided into two categories: (1) Define the delay difference between channels in the selected frequency point as the group delay mismatch level of the entire band [22–25]. (2) Define the in-band group delay difference between channels as the group delay mismatch level of the system [21, 26–29]. Furthermore, when deriving the interference cancellation performance expressions, most studies were based on the statistical characteristics of the received interference and the performance was revealed by the eigenvalues and eigenvectors from the covariance matrix [22–24, 26–33].

Since the traditional mathematical model of the adaptive interference cancellation system cannot characterize the interference bandwidth in the time domain [34], the group delay difference between channels is also difficult to be represented. Therefore, [22–25] defined the group delay mismatch of the adaptive interference cancellation system as the delay difference between channels in the selected frequency point to analyze the group delay mismatch effect on the interference cancellation performance. However, when the adaptive interference cancellation system processes wideband interference, the effect of group delay difference between channels on interference cancellation performance is unneglectable [21]. To analyze the group delay mismatch effect on interference cancellation performance, [21, 26–29] utilized the algebraic expression to characterize the interference bandwidth and group delay mismatch qualitatively and then designed the variable fractional delay FIR filter, etc., to decrease the group delay mismatch level between channels. But the mathematical models in [21, 26–29] have not quantitatively characterized the interference bandwidth, thereafter, the group delay mismatch cannot be quantitatively represented in the time domain. Thus, the effect of group delay mismatch on WIC performance can only be qualitatively analyzed and optimized.

For the interference cancellation performance analysis method, [22–24, 26–33] utilized the statistical characteristics of the received interference to derive the expressions of WIC performance. The process implicates the interference bandwidth, group delay mismatch, etc., into the eigenvalues and eigenvectors of the covariance matrix. Making it difficult to quantitatively analyze the group delay mismatch effect on the anti-jamming capability, thus, cannot provide theoretical guidance on the constraints of group delay mismatch when implementing the adaptive interference cancellation system. Therefore, an analysis method is required to characterize the interference bandwidth and group delay mismatch in the analytic expressions when implementing the adaptive interference cancellation system, thereby achieving the quantitative analysis of the group delay mismatch effect on the WIC performance.

Being motivated to quantitatively analyze the group delay mismatch effect on the hostile interference cancellation, in this paper, the mathematical model of the wideband adaptive spatial interference cancellation (ASIC) system is established. The mathematical model characterizes the interference bandwidth and group delay mismatch in the time domain, which can reflect the in-band group delay mismatch level. The performance analysis derives the analytic equations of the weight characteristics and the interference cancellation ratio (ICR), which is capable of quantitatively analyzing the group delay mismatch effect on the wideband ASIC system. The main contributions of this study are summarized as follows.

(1) The mathematical model of the wideband ASIC system is established, which can characterize the interference bandwidth and the group delay mismatch in the time domain. Utilize the weighted multi-tone signals to fit the wideband interference, and then, the delay differences are attached to each tone signal to simulate the group delay mismatch, which can accurately depict the wideband ASIC system with group delay mismatch.
(2) The quantitative analysis of the group delay mismatch effect on the wideband ASIC system is achieved, in which the interference bandwidth and group delay mismatch are directly embodied in analytic equations of weight and ICR instead of implicated in the eigenvalues and eigenvectors. The analysis results provide the quantitative relationship of the group delay mismatch with the weight and the WIC performance. For example: (A) Under fixed interference bandwidth, received interference's delay difference, and the group delay mismatch level, the weight value in steady state is accurately calculated. (B) The mean difference of group delay introduced by the main and auxiliary channels is equivalent to changing the received interference's delay difference. (C) When the ICR deterioration tolerance is less than 10 dB, the variance of the group delay fluctuation difference cannot exceed $0.2829(10\text{ps})^2$.
(3) The correctness of the proposed mathematical model and quantitative analysis results are verified through extensive simulations. For instance: (A) The convergence values and variety trend of weight are consistent in analysis and simulation results. (B) The ICR differences between analysis and simulation results under different group delay mismatch levels are all within 0.5 dB.

2 Mathematical model and performance analysis

This section establishes the mathematical model of the wideband ASIC system with group delay mismatch in the time domain. Thereafter, quantitative analysis based on the mathematical model is conducted on the weight characteristics and the WIC performance.

Since there are communication gaps in time division multiple access (TDMA) based communication systems, in which without desired signals [35], or utilize the sideband interference to obtain the sampling signal [36], the weight calculation can be conducted when no desired signal exists. Moreover, the study in this paper is carried out based on the radar or communication systems that encounter barrage jamming with a high interference-to-noise ratio (INR). Therefore, the desired signal, environmental noise, and thermal noise are not introduced in the derivation of the mathematical model.

The structure of the wideband ASIC system is shown in Fig. 1. Barrage jamming in spatial is firstly received by the main and the auxiliary antennas, in which the main antenna is the transceiver antenna of the original system, and the auxiliary antenna is the interference sampling antenna. Then, the received interference is filtered, amplified, and down-converted before input into the digital circuit for anti-jamming processing, in which the weight algorithm is probably least mean square (LMS), recursive least square (RLS), or the other algorithms. Finally, feedback the processed signal to the original system. The transmission delay and the in-band group delay fluctuation differences consist of the group delay mismatch problem in the wideband ASIC system.

2.1 Mathematical model of wideband ASIC system with group delay mismatch

In this subsection, the mathematical model of the wideband ASIC system, which considers group delay mismatch, is established. According to the FT theory, both the periodic signal

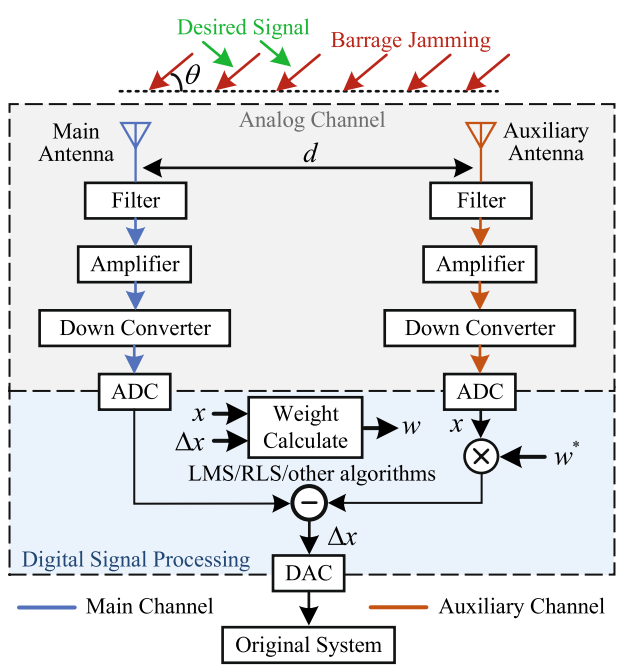

Fig. 1 Structure of the wideband ASIC system

and the aperiodic signal can be expressed as a linear combination of a group of complex exponential signals [37]. Therefore, the wideband interference can be fitted by multi-tone signals when the frequency interval is small enough. The received wideband interference in the main antenna can be expressed as

$$x = \sum_{n=1}^{N} x_n, \tag{1}$$

in which $x_n = a_n e^{j2\pi f_n t + \varphi_n}$, subscript n represents the serial number of the frequency f_n, a_n is the amplitude of the tone signal x_n, φ_n is the initial phase of the tone signal x_n, and N is the number of tone signals.

From Fig. 1, the delay difference of the received interference between the main and auxiliary antennas can be calculated by

$$\tau = d \sin\theta / \mathrm{c}, \tag{2}$$

in which $-180° \leq \theta \leq 180°$ is the angle between the interference arrival direction and the normal direction, d is the distance between main and auxiliary antennas, and c represents the transmission speed of the signal.

Then, the received wideband interference in the auxiliary antennas can be expressed as

$$x_{\mathrm{a}} = \sum_{n=1}^{N} x_n \exp\left(j\omega_n \tau\right). \tag{3}$$

The group delays in the main and auxiliary channels are defined as $\tau_{\mathrm{M}n}$ and $\tau_{\mathrm{A}n}$, including the transmission path delay and the group delay fluctuation in-band introduced by the nonlinearity of the devices in channels. References [38, 39] indicated that the group delay mismatch follows the Gaussian distribution. Therefore, this paper utilizes the Gaussian distribution to fit the group delay mismatch. The group delay variation in-band before and after passing through the main and auxiliary channels is shown in Fig. 2. Thus, the wideband interference after passing through the main and auxiliary channels can be written as

$$X_{\mathrm{M}} = \sum_{n=1}^{N} x_n \exp\left(j\omega_n \tau_{\mathrm{M}n}\right), \tag{4}$$

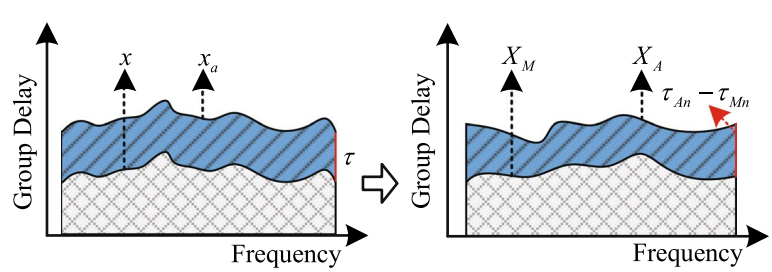

Fig. 2 The group delay variation in-band before and after passing through the main and auxiliary channels

$$X_{\mathrm{A}} = \sum_{n=1}^{N} x_n \exp\left[j\omega_n(\tau + \tau_{\mathrm{A}n})\right]. \tag{5}$$

Weight X_{A} by w_{o}, and then subtract $w_{\mathrm{o}}X_{\mathrm{A}}$ from X_{M} to obtain the error as

$$\Delta x = X_{\mathrm{M}} - w_{\mathrm{o}}X_{\mathrm{A}} = \sum_{n=1}^{N} x_n \exp\left(j\omega_n\tau_{\mathrm{M}n}\right) - w_{\mathrm{o}}\sum_{n=1}^{N} x_n \exp\left[j\omega_n(\tau + \tau_{\mathrm{A}n})\right]. \tag{6}$$

Assume that (1) the received signal in the main and auxiliary antennas has the same amplitude, and (2) the weight w_{o} in steady state is a constant, which can be written as $w_{\mathrm{o}} = k_{\mathrm{o}}e^{-j\omega_{\mathrm{o}}\tau}$. Substitute the weight into Eq. (6), the error can be rewritten as

$$\Delta x = \sum_{n=1}^{N} x_n\left(\exp\left(j\omega_n\tau_{\mathrm{M}n}\right) - k_{\mathrm{o}}\exp\left(j((\omega_n - \omega_{\mathrm{o}})\tau + \omega_n\tau_{\mathrm{A}n})\right)\right). \tag{7}$$

The adaptive control of the weight algorithm is to minimize the error power by searching for the optimal weight [12]. Assume that the amplitude of each single-tone signal is 1V. The minimum error power can be expressed as

$$\begin{aligned}\min_{\omega_{\mathrm{o}}\ k_{\mathrm{o}}} \sum_{n=1}^{N} |\Delta x_n|^2 &= \min_{\omega_{\mathrm{o}}\ k_{\mathrm{o}}} \sum_{n=1}^{N} \left|x_n\left(\exp\left(j\omega_n\tau_{\mathrm{M}n}\right) - k_{\mathrm{o}}\exp\left(j((\omega_n - \omega_{\mathrm{o}})\tau + \omega_n\tau_{\mathrm{A}n})\right)\right)\right|^2 \\ &= \min_{\omega_{\mathrm{o}}\ k_{\mathrm{o}}} \sum_{n=1}^{N} \left(1 + k_{\mathrm{o}}^2 - 2k_{\mathrm{o}}\cos\theta_n\right),\end{aligned} \tag{8}$$

in which Δx_n is the error of nth tone signal after cancellation, $\theta_n = \omega_n(\tau_{\mathrm{M}n} - \tau_{\mathrm{A}n} - \tau) + \omega_{\mathrm{o}}\tau$.

The ICR of the wideband ASIC systems is defined as

$$\mathrm{ICR} = \sum_{n=1}^{N} |x_n|^2 / \sum_{n=1}^{N} |\Delta x_n|^2 = N / \sum_{n=1}^{N} \left(1 + k_{\mathrm{o}}^2 - 2k_{\mathrm{o}}\cos\theta_n\right). \tag{9}$$

The aforementioned mathematical model of the wideband ASIC system characterizes the interference bandwidth and the group delay mismatch in the time domain, which can be applied for the quantitative analysis of the group delay mismatch effect on the weight characteristic and WIC performance.

2.2 Quantitative analysis of group delay mismatch effect on weight characteristic

In this subsection, the quantitative analysis of the weight characteristics is conducted based on the mathematical model. And the weight characteristics are divided into weight phase characteristic and weight amplitude characteristic for analysis.

2.2.1 Optimal weight phase

Calculate the partial derivative of Eq. (8) with respect to ω_{o} as

$$\begin{aligned}\sum_{n=1}^{N}|\Delta x_n|^2/\partial\omega_{\mathrm{o}} &= \sum_{n=1}^{N}\left(1+k_{\mathrm{o}}^2-2k_{\mathrm{o}}\cos\theta_n\right)/\partial\omega_{\mathrm{o}}\\ &= \sum_{n=1}^{N}2k_{\mathrm{o}}\tau\sin\theta_n.\end{aligned} \tag{10}$$

Set Eq. (10) to zero, there is

$$\sum_{n=1}^{N}2k_{\mathrm{o}}\tau\sin\theta_n = 0. \tag{11}$$

The correlation between the received interference by the main and auxiliary antennas is decreased with the enlarge of distance, and auxiliary antennas are generally arranged within $0.5\lambda \sim 2\lambda$ relative to the main antenna [40–44]. Set the highest frequency of the wideband interference as 1 GHz, the auxiliary antenna is arranged within 0.6 m relative to the main antenna, and assume that the group delay fluctuations are within 100 ps. Then, when the interference bandwidth is less than 20 MHz, there are $\tau \leq 2$ns, $(\omega_n - \omega_{\mathrm{o}}) \leq 2\pi \times 20$ MHz, and thus,

$$\theta_n \leq 0.4513. \tag{12}$$

Thus, based on the Taylor expansion of $\sin x$, Eq. (11) can be approximated as

$$\begin{aligned}\sum_{n=1}^{N}2k_{\mathrm{o}}\tau\sin\theta_n &\approx \sum_{n=1}^{N}2k_{\mathrm{o}}\tau\theta_n\\ &= \sum_{n=1}^{N}2k_{\mathrm{o}}\tau(\omega_n(\tau_{\mathrm{M}n}-\tau_{\mathrm{A}n}-\tau)+\omega_{\mathrm{o}}\tau) = 0.\end{aligned} \tag{13}$$

The optimal equivalent angular frequency of weight is

$$\omega_{\mathrm{o}} = \sum_{n=1}^{N}\omega_n(\tau+\tau_{\mathrm{A}n}-\tau_{\mathrm{M}n})/\sum_{n=1}^{N}\tau. \tag{14}$$

Assume that the received interference by main and auxiliary antennas has the same amplitude in each frequency point, thereafter, Eq. (14) can be simplified to obtain the optimal equivalent angular frequency of weight as

$$\omega_{\mathrm{o}} = \sum_{n=1}^{N}\omega_n(\tau+\tau_{\mathrm{A}n}-\tau_{\mathrm{M}n})/N\tau. \tag{15}$$

The optimal weight phase is

$$\mathrm{Pha} = \sum_{n=1}^{N}\omega_n(\tau+\tau_{\mathrm{A}n}-\tau_{\mathrm{M}n})/N. \tag{16}$$

According to Eqs. (15) and (16), the optimal weight phase is relevant to the delay difference between the received interference by main and auxiliary antennas τ, and the group

delay differences introduced by the main and auxiliary channels $\tau_{\mathrm{A}n} - \tau_{\mathrm{M}n}$. It can be drawn that

(1) When the group delay differences $\tau_{\mathrm{A}n} - \tau_{\mathrm{M}n}$ introduced by the main and auxiliary channels are zero, the optimal equivalent angular frequency of weight converges to the center angular frequency of the interference. And the optimal weight phase converges to the equal phase in the center frequency of interference $\sum_{n=1}^{N} \omega_n \tau / N$.

(2) When the group delay differences $\tau_{\mathrm{A}n} - \tau_{\mathrm{M}n}$ introduced by the main and auxiliary channels are not zero, the optimal equivalent angular frequency and phase of weight deviate from the center frequency. Thereafter, affecting the WIC performance cannot be compensated by limited amount weights.

2.2.2 Optimal weight amplitude

Calculate the partial derivative of Eq. (8) with respect to k_{o} as

$$\begin{aligned} \sum_{n=1}^{N} |\Delta x_n|^2 / \partial k_{\mathrm{o}} &= \sum_{n=1}^{N} \left(1 + k_{\mathrm{o}}^2 - 2k_{\mathrm{o}} \cos\theta_n\right) / \partial k_{\mathrm{o}} \\ &= \sum_{n=1}^{N} 2(k_{\mathrm{o}} - \cos\theta_n). \end{aligned} \tag{17}$$

Set Eq. (17) to zero, the optimal weight amplitude is obtained as

$$\begin{aligned} \sum_{n=1}^{N} |\Delta x_n|^2 / \partial k_{\mathrm{o}} &= \sum_{n=1}^{N} 2(k_{\mathrm{o}} - \cos\theta_n) = 0 \\ &\Rightarrow k_{\mathrm{o}} = \sum_{n=1}^{N} \cos\theta_n / N, \end{aligned} \tag{18}$$

in which $\theta_n = \omega_n(\tau_{\mathrm{M}n} - \tau_{\mathrm{A}n} - \tau) + \omega_{\mathrm{o}}\tau$.

From Eq. (12), $\theta_n \leq 0.4513$, then based on the Taylor expansion of $\cos x$, Eq. (18) can be approximated as

$$k_{\mathrm{o}} \approx 1. \tag{19}$$

According to Eqs. (18) and (19), the group delay differences $\tau_{\mathrm{A}n} - \tau_{\mathrm{M}n}$ introduced by the main and auxiliary channels also affect the convergence value of the weight amplitude. However, the effect is slight, and the weight amplitude approximately converges to 1.

Based on the analysis above of the weight characteristics, it can be drawn that

(1) The group delay differences $\tau_{\mathrm{A}n} - \tau_{\mathrm{M}n}$ introduced by the main and auxiliary channels affect the convergence values of weight phase and amplitude. Moreover, since the $\tau_{\mathrm{A}n} - \tau_{\mathrm{M}n}$ is related to the frequency, which cannot be compensated by limited amount weights, it will directly impact the anti-jamming performance of the wideband ASIC system.

(2) When the interference bandwidth N, the delay difference τ between the received interference by main and auxiliary antennas, and the group delay differences $\tau_{\mathrm{A}n} - \tau_{\mathrm{M}n}$ introduced by the main and auxiliary channels are known, the convergence values of weight phase and amplitude can be calculated in theory. Therefore, based on the mathematical model proposed in this paper, the quantitative analysis of weight characteristics is realized. Thereafter, the theoretical analysis will be verified through simulation in Sect. 3.

2.3 Quantitative analysis of group delay mismatch effect on WIC performance

Substitute Eqs. (8), (16), and (18) into Eq. (9), the analytical expression of ICR that considers the group delay mismatch can be expressed as

$$\mathrm{ICR} = N / \left(\sum_{n=1}^{N} \left(1 + \left(\sum_{n=1}^{N} \cos\theta_n / N \right)^2 - 2\cos\theta_n \sum_{n=1}^{N} \cos\theta_n / N \right) \right). \tag{20}$$

And substitute Eq. (16) into θ_n, it can be expressed as

$$\theta_n = \omega_n(\tau_{\mathrm{M}n} - \tau_{\mathrm{A}n} - \tau) - \sum_{n=1}^{N} \omega_n(\tau_{\mathrm{M}n} - \tau_{\mathrm{A}n} - \tau)/N. \tag{21}$$

From Eqs. (20) and (21), it can be drawn that since the group delay differences $\tau_{\mathrm{A}n} - \tau_{\mathrm{M}n}$ introduced by the main and auxiliary channels are related to the frequency, that cannot be compensated by limited amount weights. It will directly affect the ICR of the wideband ASIC system.

To quantitatively analyze the group delay mismatch effect on the wideband ASIC system, the group delay difference $\tau_{\mathrm{A}n} - \tau_{\mathrm{M}n}$ is divided into mean difference $\mathrm{mean}(\tau_{\mathrm{A}n} - \tau_{\mathrm{M}n})$ and zero mean fluctuation $\tau_{\mathrm{A}n} - \tau_{\mathrm{M}n} - \mathrm{mean}(\tau_{\mathrm{A}n} - \tau_{\mathrm{M}n})$ for analysis, respectively. Theoretical analysis results calculated by Eqs. (20) and (21) are shown in Fig. 3

From Fig. 3, the quantitative analysis results of the group delay mismatch effect on ICR can be drawn as

(1) The mean difference of group delay $\mathrm{mean}(\tau_{\mathrm{A}n} - \tau_{\mathrm{M}n})$ introduced by the main and auxiliary channels is equivalent to changing the delay difference τ between the received interference by main and auxiliary antennas. As shown in Fig. 3a, the optimal ICR is obtained when the mean difference of group delay $\mathrm{mean}(\tau_{\mathrm{A}n} - \tau_{\mathrm{M}n})$ is equal to the negative of the delay difference τ. However, it will decrease the spatial resolution of the array manifold; meanwhile, $\mathrm{mean}(\tau_{\mathrm{A}n} - \tau_{\mathrm{M}n})$ is determined by the circuit consistency which cannot be adjusted manually. Therefore, when implementing the wideband ASIC system, it is necessary to compensate for the $\mathrm{mean}(\tau_{\mathrm{A}n} - \tau_{\mathrm{M}n})$ to improve the performance of the system.
(2) Similarly, in Fig. 3a, ICR decreases when the mean difference of group delay $\mathrm{mean}(\tau_{\mathrm{A}n} - \tau_{\mathrm{M}n})$ enlarges the delay difference τ. With the increase in delay difference τ, the phase difference between channels at the boundary frequency enlarges, which results in the ICR decrease.

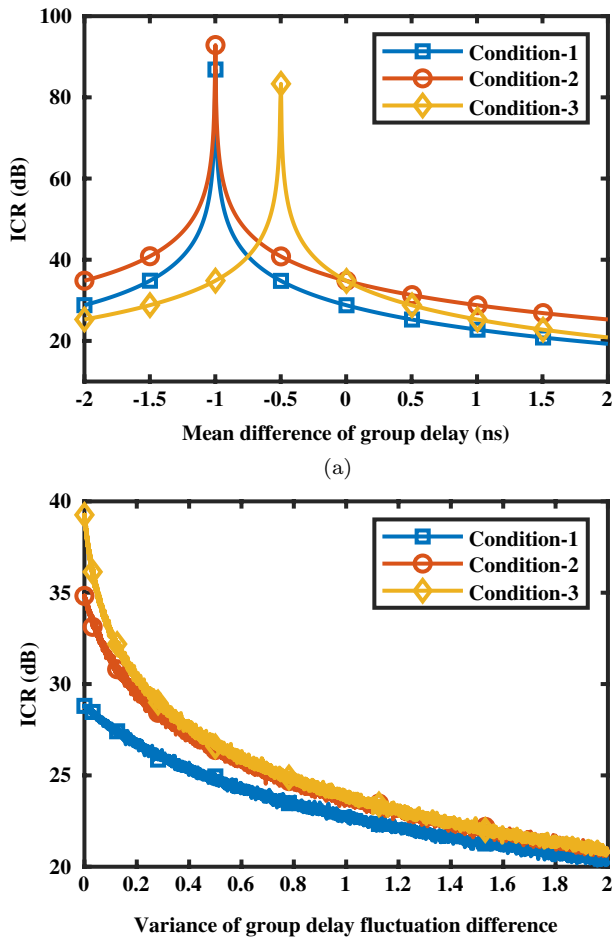

Fig. 3 Quantitative analysis results of ICR under group delay mismatch. **a** The relationship between ICR and mean difference of group delay under three conditions: (1) Condition-1 with 20 MHz interference bandwidth, and 1 ns delay difference. (2) Condition-2 with 10 MHz interference bandwidth, and 1 ns delay difference. (3) Condition-3 with 20 MHz interference bandwidth, and 0.5 ns delay difference. **b** The relationship between ICR and zero mean fluctuation of group delay under three conditions: (1) Condition-1 with 20 MHz interference bandwidth, and 1 ns delay difference. (2) Condition-2 with 10 MHz interference bandwidth, and 1 ns delay difference. (3) Condition-3 with 20 MHz interference bandwidth, and 0.3 ns delay difference.

(3) As shown in Fig. 3b, the group delay fluctuation differences $\tau_{\mathrm{A}n} - \tau_{\mathrm{M}n} - \mathrm{mean}(\tau_{\mathrm{A}n} - \tau_{\mathrm{M}n})$ introduced by the main and auxiliary channels directly affect the ICR of the wideband ASIC system. In condition-3, when the wideband ICR deterioration tolerance is less than 5 dB, the variance of $\tau_{\mathrm{A}n} - \tau_{\mathrm{M}n} - \mathrm{mean}(\tau_{\mathrm{A}n} - \tau_{\mathrm{M}n})$ cannot exceed $0.0706((10\mathrm{ps})^2)$. Meanwhile, when the ICR deterioration tolerance is less than 10 dB, the variance of $\tau_{\mathrm{A}n} - \tau_{\mathrm{M}n} - \mathrm{mean}(\tau_{\mathrm{A}n} - \tau_{\mathrm{M}n})$ cannot exceed $0.2829((10\mathrm{ps})^2)$. The group delay fluctuation differences under the variance of $0.0706((10\mathrm{ps})^2)$ and $0.2829((10\mathrm{ps})^2)$ are shown in Fig. 4a and b.

(4) The same in Fig. 3b, when the variance of $\tau_{\mathrm{A}n} - \tau_{\mathrm{M}n} - \mathrm{mean}(\tau_{\mathrm{A}n} - \tau_{\mathrm{M}n})$ achieves $2((10\mathrm{ps})^2)$, the ICRs under three conditions tend to be consistent. The group delay

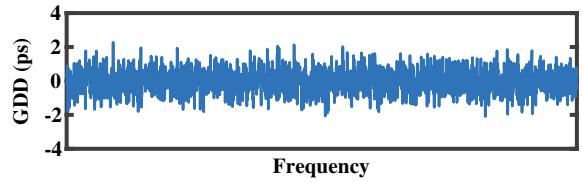

(a) Variance of group delay fluctuation difference: $0.0706((10\text{ps})^2)$

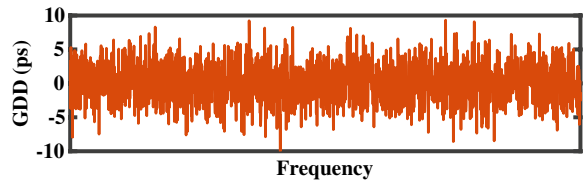

(b) Variance of group delay fluctuation difference: $0.2829((10\text{ps})^2)$

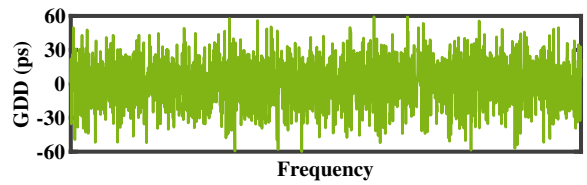

(c) Variance of group delay fluctuation difference: $2((10\text{ps})^2)$

Fig. 4 The group delay fluctuation differences under different variances

fluctuation differences under the variance of $2((10\text{ps})^2)$ are shown in Fig. 4c, which means that the group delay fluctuation differences $\tau_{\mathrm{A}n} - \tau_{\mathrm{M}n} - \mathrm{mean}(\tau_{\mathrm{A}n} - \tau_{\mathrm{M}n})$ become the main factor that affects the ICR, and the ICR improvement from decreasing the processing interference bandwidth and the delay difference τ will be consumed. Therefore, it is also necessary to compensate for the group delay fluctuation difference between the main and auxiliary channels, which can effectively improve the anti-jamming capability of the wideband ASIC system.

According to the weight characteristics and WIC performance analysis results above, it can be drawn that the group delay differences $\tau_{\mathrm{A}n} - \tau_{\mathrm{M}n}$ introduced by the main and auxiliary channels directly affect the steady-state weight and the ICR and cannot be compensated by limited amount weights. Thus, it is required for the group delay mismatch compensation in the implementation of the wideband ASIC system for the anti-jamming capability improvement.

In the actual circuit, the group delay mismatch generally accompanies the gain mismatch between the main and auxiliary channels. Thus, it is hard to individually verify the analysis results' accuracy of group delay mismatch effect on the wideband ASIC system by experiments. The correctness and accuracy of the analysis results in this Section are demonstrated by simulations, which are shown in Sect. 3.

Table 1 Simulation parameters

Parameter	Value
Interference bandwidth	10 MHz, 20 MHz
Carrier frequency	990 MHz
Interference type	Band-limited random noise
Interference amplitude in auxiliary element	1.0×-main element interference amplitude
Time delay difference	0.5 ns, 1 ns
Weight algorithm	LMS

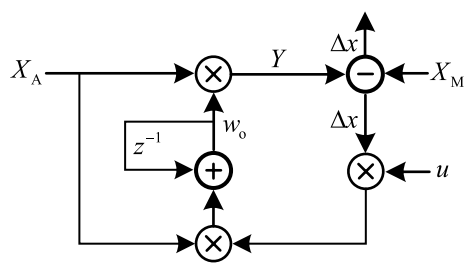

Fig. 5 Block diagram of the LMS algorithm

3 Simulation verification

In this section, extensive simulations are conducted to verify the analysis results of the group delay mismatch effect on weight characteristics and the WIC performance in Sect. 2. The simulation parameters are shown in Table 1, similarly assuming that the group delay fluctuation difference between channels follows the Gaussian distribution.

The least mean square (LMS) is a typical adaptive algorithm of weight calculation by searching the optimal weight to minimize the square of the error signal [45]. The block diagram of the LMS algorithm is shown in Fig. 5. The weight calculation steps based on the LMS algorithm can be expressed as

$$Y(n) = w(n)X_A(n), \tag{22}$$

$$\Delta x(n) = X_M(n) - Y(n), \tag{23}$$

$$w(n+1) = w(n) + u\Delta x(n)X_A(n), \tag{24}$$

where u is the constant to adjust the calculation step, and the step size in the simulation is fixed to 0.5.

3.1 Simulation of weight characteristics under group delay mismatch

The weight characteristics determine the WIC performance of the wideband ASIC system. In this subsection, analysis and simulation results of weight characteristics are compared to verify the quantitative analysis's accuracy of the group delay mismatch effect in Sect. 2. Set the interference bandwidth as 20MHz, and the delay difference τ between the received interference by main and auxiliary antennas as 1ns. Thereafter, the analysis and

Table 2 Analysis (AR) and simulation (SR) results comparison of the weight characteristics in which M-GDM is the mean of $\tau_{An} - \tau_{Mn}$ (ns), and V-GDM is the variance of $\tau_{An} - \tau_{Mn} - \text{mean}(\tau_{An} - \tau_{Mn})((10\text{ps})^2)$

Condition	M-GDM	V-GDM	AR-amplitude	AR-phase	SR-amplitude	SR-phase
COND-1	0	0	0.999	0.0618	0.999	0.0614
COND-2	0	0.2	0.999	0.0628	0.999	0.0624
COND-3	0	1	0.997	0.063	0.996	0.0644
COND-4	0.5	0	0.999	− 3.047	1	− 3.049
COND-5	0.5	0.2	0.998	− 3.05	0.999	− 3.051
COND-6	0.5	1	0.997	− 3.048	0.995	− 30.46
COND-7	− 0.5	0	1	− 3.11	0.998	− 3.11
COND-8	− 0.5	0.2	0.999	− 3.109	0.998	− 3.109
COND-9	− 0.5	1	0.998	− 3.047	0.997	− 3.114

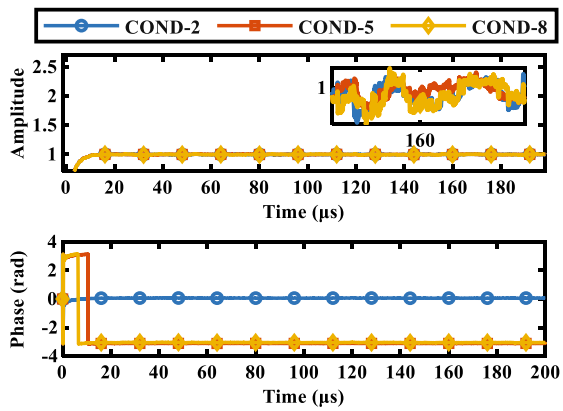

(a) mean $(\tau_{An} - \tau_{Mn})$ effect on the weight characteristics

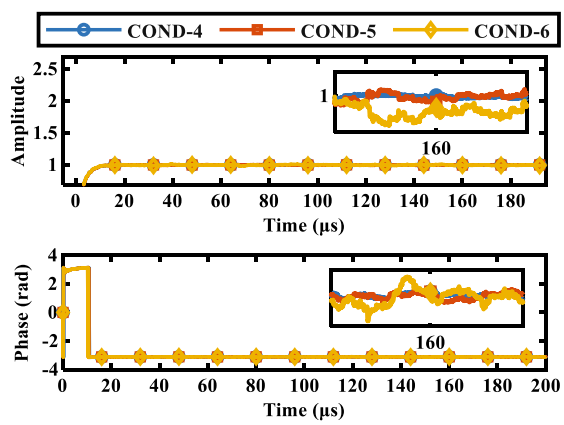

(b) $\tau_{An} - \tau_{Mn} - \text{mean}(\tau_{An} - \tau_{Mn})$ effect on the weight characteristics

Fig. 6 Simulation results of the group delay mismatch effect on weight characteristics

simulation results of weight characteristics based on the above parameters are compared in Table 2, in which the analysis results are calculated by Eqs. (16) and (18). Furthermore, the weight convergence process in the simulation is shown in Fig. 6.

From the simulation and analysis results above, it can be drawn that

(1) Compare the simulation and analysis results of weight amplitude in Table 2, the group delay mismatch slightly affects the steady-state weight. The weight amplitudes and phases in steady state are consistent in simulation and analysis results under different group delay mismatch levels, which means that the proposed mathematical model of the wideband ASIC system can accurately characterize the group delay mismatch effect on the weight characteristics.
(2) From Table 2 and Fig. 6a, the mean difference of group delay $\mathrm{mean}(\tau_{\mathrm{A}n} - \tau_{\mathrm{M}n})$ makes the weight deviate from the optimal value, which is consistent with the analysis results. The $\mathrm{mean}(\tau_{\mathrm{A}n} - \tau_{\mathrm{M}n})$ decreases the spatial resolution of the array manifold and will affect the anti-jamming capability of the wideband ASIC system.
(3) From Fig. 6b, the fluctuation of steady-state weight enlarges with the variance of group delay fluctuation difference increase, which will directly affect the wideband ASIC system's ICR.

The consistency in simulation and analysis results proves that the proposed mathematical model of the wideband ASIC system can quantitatively analyze the group delay mismatch effect on the system's weight characteristics.

3.2 Simulation of WIC performance under group delay mismatch

Extensive simulations are conducted in this subsection under different group delay mismatch levels to verify the quantitative analysis results of the group delay mismatch effect on the WIC performance in Sect. 2.

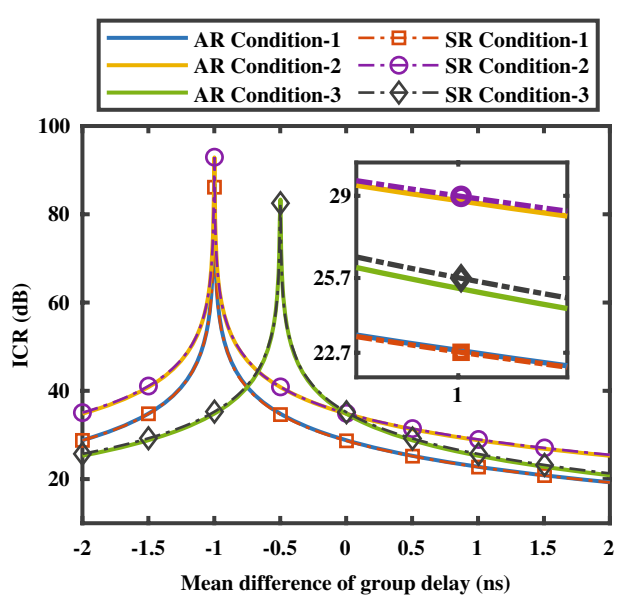

Fig. 7 Comparison of simulation (SR) and analysis results (AR) of the relationship between ICR and mean difference of group delay under three conditions: (1) Condition-1 with 20MHz interference bandwidth, and 1ns delay difference. (2) Condition-2 with 10MHz interference bandwidth, and 1ns delay difference. (3) Condition-3 with 20MHz interference bandwidth, and 0.5ns delay difference

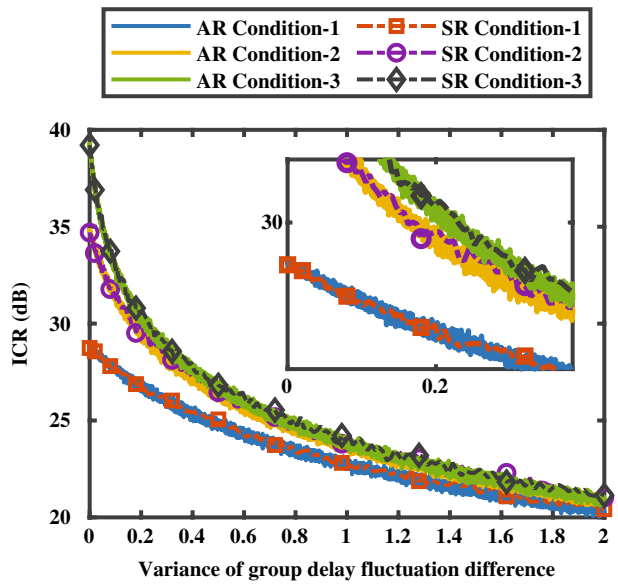

Fig. 8 Comparison of simulation (SR) and analysis results (AR) of the relationship between ICR and zero mean fluctuation of group delay under three conditions: (1) Condition-1 with 20MHz interference bandwidth, and 1ns delay difference. (2) Condition-2 with 10MHz interference bandwidth, and 1ns delay difference. (3) Condition-3 with 20MHz interference bandwidth, and 0.3ns delay difference

The same as in Sect. 2.3, divide the group delay differences $\tau_{\mathrm{A}n} - \tau_{\mathrm{M}n}$ introduced by the main and auxiliary channels into mean difference $\mathrm{mean}(\tau_{\mathrm{A}n} - \tau_{\mathrm{M}n})$ and zero mean fluctuation $\tau_{\mathrm{A}n} - \tau_{\mathrm{M}n} - \mathrm{mean}(\tau_{\mathrm{A}n} - \tau_{\mathrm{M}n})$ to simulate the effect on the ICR. The simulation results of the group delay mismatch effect on the ICR under different parameters are shown in Figs. 7 and 8.

From Figs. 7 and 8, the simulation results of group delay mismatch effect on the ICR are consistent with the analysis results, in which the differences are within 0.5 dB. The consistency proves that the proposed mathematical model of the wideband ASIC system can accurately and quantitatively analyze the group delay mismatch effect on the WIC performance and, thereafter, provide theoretical guidance for the constraint of the group delay consistent when implementing the wideband ASIC system.

4 Conclusion

This paper established a time domain mathematical model of wideband ASIC system to quantitatively analyze the group delay mismatch effect on the weight characteristics and the WIC performance. The mathematical model characterizes the group delay mismatch in the time domain, which can accurately depict the wideband ASIC system with group delay mismatch. Thereafter, the analytical expressions of weight characteristics and the WIC performance are obtained based on the mathematical model, which achieve the quantitative analysis of the group delay mismatch effect on the wideband ASIC system. The main conclusions are drawn below:

(1) The mean difference of group delay mismatch $\mathrm{mean}(\tau_{\mathrm{A}n} - \tau_{\mathrm{M}n})$, which is introduced by the main and auxiliary channels, makes the weight phase in steady state deviate from the optimal value and affects the spatial resolution of the array

manifold. Thus, when designing and implementing the wideband ASIC system, it is required to compensate for the mean difference of group delay mismatch to decrease the effect on system performance.

(2) The group delay fluctuation differences $\tau_{\mathrm{A}n} - \tau_{\mathrm{M}n} - \mathrm{mean}(\tau_{\mathrm{A}n} - \tau_{\mathrm{M}n})$ are related to the frequency, which cannot be compensated by limited amount weights. Moreover, the fluctuation of steady-state weight enlarges with the variance of $\tau_{\mathrm{A}n} - \tau_{\mathrm{M}n} - \mathrm{mean}(\tau_{\mathrm{A}n} - \tau_{\mathrm{M}n})$ increases, which will directly affect the ICR of the wideband ASIC system. For example, when the ICR deterioration tolerance is less than 10 dB, the variance of $\tau_{\mathrm{A}n} - \tau_{\mathrm{M}n} - \mathrm{mean}(\tau_{\mathrm{A}n} - \tau_{\mathrm{M}n})$ cannot exceed $0.2829((10\mathrm{ps})^2)$(delay difference: $\tau = 0.3ns$, interference bandwidth: 20 MHz).

(3) Simulation results verify the correctness and accuracy of the wideband ASIC system's mathematical model, which considers the group delay mismatch. For instance: (A) The convergence values and variety trend of weight are consistent in analysis and simulation results. (B) The ICR differences between analysis and simulation results under different group delay mismatch levels are all within 0.5 dB.

The conclusions above prove that the wideband ASIC system's mathematical model proposed in this paper is capable of accurately and quantitatively analyzing the group delay mismatch effect on the weight characteristics and WIC performance and, thereafter, provides effective guidance when designing the group delay constraint in channels.

Acknowledgements
Not applicable.

Author contributions
FH and YZ contributed to conceptualization and writing—review and editing, and provided software; YZ was involved in data curation; FH and HL contributed to formal analysis; YZ, YL, and ZW were involved in investigation and validation; YZ and ZY contributed to methodology; FH and JM were involved in project administration; FH, HL, and JM contributed to resources and supervision; and YZ was involved in writing—original draft. All authors have read and agreed to the published version of the manuscript.

Funding
This work was partially supported by the National Key R &D Program of China under Grant 2021YFF1500100, the National Science Fund for Distinguished Young Scholars under Grant 52025072, the National Natural Science Foundation of China under Grants 52177012 and 62271497, and the Natural Science Foundation of Hubei Province under Grant 2021BIDS007.

Availability of data and materials
All data generated during this study are included in this published article.

Declarations

Ethics approval and consent to participate
Not applicable.

Consent for publication
Not applicable.

Competing interests
The authors declare that they have no competing interests.

Received: 4 May 2023 Accepted: 19 September 2023
Published online: 26 September 2023

References

1. V.T. Klingelfus, A.L.C. Serrano, G.P. Rehder, Co-site interference study and mitigation onboard a submarine between communication and positioning systems at l band. IEEE Lett. Electromag. Compat. Pract. Appl. **3**(1), 38–42 (2021)
2. S. Ge, J. Meng, J. Xing, Y. Liu, C. Gou, A digital-domain controlled nonlinear RF interference cancellation scheme for co-site wideband radios. IEEE Trans. Electromagn. Compat. **61**(5), 1647–1654 (2019)

3. S. Cheng, X. Sun, Y. Cai, H. Zheng, W. Yu, Y. Zhang, S. Chang, A joint azimuth multichannel cancellation (JAMC) anti-barrage jamming scheme for spaceborne SAR. IEEE J. Sel. Top. Appl. Earth Obs. Remote Sens. **15**, 9913–9926 (2022)
4. Z. Luo, K. Lu, X. Chen, Z. He, Wideband signal design for over-the-horizon radar in cochannel interference. EURASIP J. Adv. Signal Process. **2014**, 159 (2014)
5. K. Yuto, S. Yohei, O. Tomoaki, M. Jun, Suppression of multiple wideband interferences based on superposition probability. EURASIP J. Wirel. Commun. Netw. **2016**, 198 (2016)
6. X. Chen, T. Shu, K.-B. Yu, Y. Zhang, Z. Lei, J. He, W. Yu, Implementation of an adaptive wideband digital array radar processor using subbanding for enhanced jamming cancellation. IEEE Trans. Aerosp. Electron. Syst. **57**(2), 762–775 (2021)
7. Elezi, E., Çankaya, G., Boyacı, A., Yarkan, S.: The effect of electronic jammers on GPS signals, in *2019 16th International Multi-Conference on Systems, Signals and Devices (SSD)* (2019), pp. 652–656
8. L. Lightfoot, L. Zhang, J. Ren, T. Li, Secure collision-free frequency hopping for OFDMA-based wirelessnetworks. EURASIP J. Adv. Signal Process. **2009**, 361063 (2009)
9. M.M. Olama, X. Ma, S.M. Killough, T. Kuruganti, S.F. Smith, S.M. Djouadi, Analysis, optimization, and implementation of a hybrid DS/FFH spread-spectrum technique for smart grid communications. EURASIP J. Adv. Signal Process. **2015**, 25 (2015)
10. W. Mei, *Data Link of JTIDS/Link16* (National Defense Industry Press, Beijing, 2007)
11. I Gao, S. Chen, L. Jiang, Q. Li, Current situation and technique development trends of us navy ew system. Flight Control Detect. **5**(4), 35–43 (2022)
12. X. Yang, *Performance of Adaptive Arrays in Jamming Environments* (National Defense Industry Press, Beijing, 2022)
13. F. Yao, *Communication Anti-jamming Engineering and Practice* (Publishing House of Electronics Industry, Beijing, 2008)
14. H. Qin, J. Meng, F. He, Q. Wang, B. Li, Design and analysis of digital-to-analog hybrid RF interference cancellation system based on multitap structure. IEEE Trans. Microw. Theory Tech. **69**(9), 4300–4314 (2021)
15. Y. Zhang, Q. Wang, H. Qin, F. He, J. Meng, Stability improvement of analog adaptive self-interference cancellation system with phase compensation. Electromagn. Res. C **95**, 227–238 (2019)
16. W. Bernard, D.S. Samuel, *Adaptive Signal Processing* (Pearson Education, USA, 1985)
17. S. Dai, M. Li, Q.H. Abbasi, M.A. Imran, A fast blocking matrix generating algorithm for generalized sidelobe canceller beamformer in high speed rail like scenario. IEEE Sens. J. **21**(14), 15775–15783 (2021)
18. K. Duan, H. Xu, H. Yuan, H. Xie, Y. Wang, Reduced-DOF three-dimensional STAP via subarray synthesis for non-sidelooking planar array airborne radar. IEEE Trans. Aerosp. Electron. Syst. **56**(4), 3311–3325 (2020)
19. J. Liu, N. Khaled, F. Petré, A. Bourdoux, A. Barel, Impact and mitigation of multiantenna analog front-end mismatch in transmit maximum ratio combining. EURASIP J. Adv. Signal Process. **2006**, 086931 (2006)
20. Y.S. Poberezhskiy, G.Y. Poberezhskiy, Flexible analog front ends of reconfigurable radios based on sampling and reconstruction with internal filtering. EURASIP J. Wirel. Commun. Netw. **2005**, 381832 (2005)
21. C. Li, H. Zhao, F. Wu, Y. Tang, Digital self-interference cancellation with variable fractional delay fir filter for full-duplex radios. IEEE Commun. Lett. **22**(5), 1082–1085 (2018)
22. H. Qin, F. He, J. Meng, Q. Wang, Analysis and optimal design of radio-frequency interference adaptive cancellation system with delay mismatch. IEEE Trans. Electromagn. Compat. **61**(6), 2015–2023 (2019)
23. T. Su, F. Li, Z. Lian, Z. Feng, Y. Li, Z. Liu, Frequency shift of ring oscillators due to radio frequency interference on the supply. IEEE Trans. Electromagn. Compat. **57**(6), 1365–1373 (2015)
24. K. Kim, A.A. Iliadis, Impact of microwave interference on dynamic operation and power dissipation of CMOS inverters. IEEE Trans. Electromagn. Compat. **49**(2), 329–338 (2007)
25. Y. Chen, J. Zhang, A.D.S. Jayalath, Low-complexity estimation of cfo and frequency independent i/q mismatch for ofdm systems. EURASIP Journal on Wireless Communications and Networking **2009**(542187), (2009)
26. W. Li, J. Meng, J. Tang, F.-M. He, Y. Li, Interference cancellation system instantaneous bandwidth and time delay problem research, in 2022 Asia-Pacific International Symposium on Electromagnetic Compatibility (APEMC) vol. 01 (2016), pp. 442–444
27. Q. Zou, Z.L. Yu, Z. Lin, A robust algorithm for linearly constrained adaptive beamforming. IEEE Signal Process. Lett. **11**(1), 26–29 (2004)
28. Y. Liu, C. Liu, D. Hu, Y. Zhao, Robust adaptive wideband beamforming based on time frequency distribution. IEEE Trans. Signal Process. **67**(16), 4370–4382 (2019)
29. Y. Liu, X. Quan, W. Pan, S. Shao, Y. Tang, Performance analysis of direct-learning digital predistortion with loop delay mismatch in wideband transmitters. IEEE Trans. Veh. Technol. **65**(9), 7078–7089 (2016)
30. J. He, T. Shu, V. Dakulagi, L. Li, Simultaneous interference localization and array calibration for robust adaptive beamforming with partly calibrated arrays. IEEE Trans. Aerosp. Electron. Syst. **57**(5), 2850–2863 (2021)
31. F. Yang, Analysis of unconstrained partitioned-block frequency-domain adaptive filters. IEEE Signal Process. Lett. **29**, 2377–2381 (2022)
32. Y. Zhang, K. Yang, M.G. Amin, Subband array implementations for space-time adaptive processing. EURASIP J. Adv. Signal Process. **2005**, 640351 (2005)
33. M. Zuo, S. Xie, A novel DOA estimation method for an antenna array under strong interference. EURASIP J. Adv. Signal Process. **2022**, 111 (2022)
34. C.L. Zahm, Application of adaptive arrays to suppress strong jammers in the presence of weak signals. IEEE Trans. Aerosp. Electron. Syst. AES **9**(2), 260–271 (1973)
35. N. Lv, *Theory and System of Data Link* (Publishing House of Electronics Industry, Beijing, 2018)
36. P. Rivkin, Y. Zhang, H. Wang, Spatial adaptive pre-suppression of wideband jammers in conjunction with STAP: a sideband approach, in *Proceedings of International Radar Conference* (1996), pp. 439–443
37. V.O. Alan, S.W. Alan, S.H. Nawab, *Signals and systems* (Pearson Education, USA, 2013)
38. Z. Li, L. Yan, B. Luo, W. Pan, Phase fluctuation cancellation for uplink radar arrays based on passive frequency mixing. IEEE Photonics J. **10**(2), 1–7 (2018)

39. G. Chaudhary, Y. Jeong, J. Lim, Microstrip line negative group delay filters for microwave circuits. IEEE Trans. Microw. Theory Tech. **62**(2), 234–243 (2014)
40. X. Yang, S. Li, Q. Liu, T. Long, T.K. Sarkar, Robust wideband adaptive beamforming based on focusing transformation and steering vector compensation. IEEE Antennas Wirel. Propag. Lett. **19**(12), 2280–2284 (2020)
41. D. Nguyen, M. Zomorrodi, N. Karmakar, K. Ho, Efficient beamforming technique based on sparse MIMO array and spatial filter bank. IEEE Antennas Wirel. Propag. Lett. **19**(7), 1147–1151 (2020)
42. R.L. Fante, J.J. Vaccaro, Wideband cancellation of interference in a GPS receive array. IEEE Trans. Aerosp. Electron. Syst. **36**(2), 549–564 (2000)
43. J.R. Mohammed, K.H. Sayidmarie, Sidelobe cancellation for uniformly excited planar array antennas by controlling the side elements. IEEE Antennas Wirel. Propag. Lett. **13**, 987–990 (2014)
44. W. Zhou, X. Li, H. Wu, Y. Xu, Q. Zhou, Y. Rao, Predictive precoding based on the Grassmannian manifold for UAV-enabled cache-assisted b5g communication systems. EURASIP J. Wirel. Commun. Netw. **2020**, 128 (2020)
45. S. Haykin, *Adaptive filter theory* (Pearson Education, USA, 2016)

Publisher's Note